Phase Diagram Construction for Quantum Spin Ice Under the Transverse Ising Model with Exact Diagonalization and Numerical Linked Cluster Methods

J. Jiang[1], Y.T. Zhang[2], and R.R.P. Singh[2]
[1]*Physics Department, Smith College and*
[2]*Physics Department, University of California, Davis*

We present calculations of properties at $T = 0$ of a checkerboard lattice under the Transverse Ising model using Exact Diagonalization (ED) of a 4×4 checkerboard lattice and Numerical-Linked Cluster (NLC) methods up to order six. Our results reproduce the expected behavior of the lattice for the magnetization M, the entanglement entropy S_E, the Néel state order parameter $S_{\pi,\pi}$, and the fidelity susceptibility χ_F at different values of h and J_2/J_1. Ongoing work will extend this analysis and construct a complete phase diagram for the system using these methods.

I. INTRODUCTION

In recent years, the quantum properties of frustrated magnetic systems have become a subject of strong interest. A frustrated magnetic system is a system whose geometry makes it impossible for any ordering of spins to achieve an antiferromagnetic alignment with every bond. Due to this, frustrated systems often exhibit unique behaviors in order to resolve this conflict. Importantly, frustration often gives rise to high degeneracy in the ground state with unique spin arrangements. One interesting property is that introducing quantum fluctuations in frustrated systems can lift these degeneracies and give rise to novel quantum phases such as spin liquids. These phases can exhibit unique quantum mechanical properties, such as high internal entanglement. The possibility that they could be present in real materials means that it is extremely important that they are closely studied.

One well known frustrated magnetic system is the two-dimensional spin ice lattice, commonly known as the checkerboard lattice (See Figure. 1a). Under the classical Ising Model, where nearest and next nearest neighbor bonds contribute equally (that is, the case where $J_1 = J_2$), the ground states of the two-dimensional spin ice lattice are those that obey the Pauling Ice Rules, where each of the plaquettes with cross bonds in Figure. 1a contain two up spins and two down spins (see Figure. 1b). In this case, the frustration of the lattice gives rise to high degeneracy in the ground state. However, the introduction of a quantum fluctuation– in particular, the addition of a field term to the Ising Model in the form of the Transverse Ising model (see Equation. 1)– completely lifts this degeneracy, and the ground state instead becomes a quantum superposition of the classical ground states in Fig. 1b. Furthermore, the lattice begins to exhibit additional interesting behavior when competition between the energy of the nearest neighbor and next nearest neighbor bonds arises (the case where $J_1 \neq J_2$). Thus, the Transverse Ising model on the checkerboard lattice is an excellent model system for several interesting physical systems.

Previous work using unconstrainted tree tensor network and mapping analysis has found four distinct ground state phases of the quantum spin ice system: Néel, colinear, quantum paramagnetic, and plaquette-valence solid phases [1]. For this project, we seek to confirm these phases by utilizing Exact Diagonalization techniques on a four-by-four checkerboard lattice and up to sixth order Numerical-Linked Cluster (NLC) methods to calculate properties of the system.

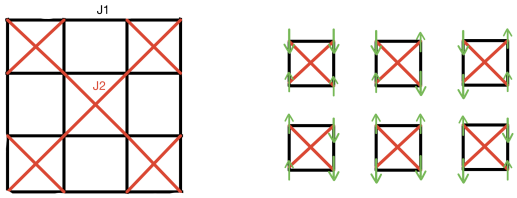

FIG. 1: 1a. The Checkerboard Lattice. J_1 represents the strength of the nearest neighbor bonds (the bonds colored in black), whereas J_2 represents the strength of the next nearest neighbor bonds (the bonds colored in red). 1b. The 6 states in a single cross plaquette that obey the Pauling Ice Rules.

II. PROCEDURE

A. The Hamiltonian

The Hamiltonian of interest is the Transverse Ising Model:

$$H = J_1 \sum_{<ij>} S_i^z S_j^z + J_2 \sum_{<<ij>>} S_i^z S_j^z + h \sum_i S_i^x \qquad (1)$$

Where $< ij >$ indicates the sites of the nearest neighbor bonds, $<< ij >>$ indicates the sites of the next nearest neighbor bonds, and i is an indication of all of the sites in the lattice. h is the strength of the quantum fluctuation, and J_1 and J_2 are the strengths of the nearest and next nearest neighbor bonds, respectively. Finally, S^z and S^x refer to the components of spin of magnitude $\frac{1}{2}$ in the z and x directions, respectively. For this problem, we apply the Hamiltonian to the spin ice lattice presented in Figure. 1a.

B. Exact Diagonalization

With Exact Diagonalization techniques, we focus on the 4×4 checkerboard lattice shown in Figure 1a. with periodic boundary conditions applied as in Figure. 2.

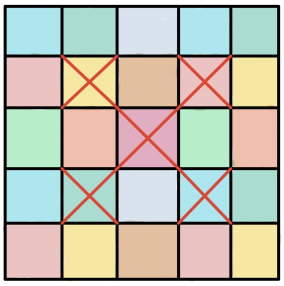

FIG. 2: The periodic boundary conditions as applied to the 4×4 checkerboard lattice. Color codes indicate which squares are identical.

Since there are 2^{16} possible configurations of spins in the lattice, the size of the Hamiltonian in this case becomes $2^{16} \times 2^{16}$. Full diagonalization of a matrix of this size (i.e. finding all of the eigenvalues and eigenvectors) is extremely difficult with the machines available, and thus we exploit symmetries in the Hamiltonian to block diagonalize the matrix and reduce the overall computational memory required. In particular, if we take the Hamiltonian in Equation. 2 and switch to the S_x basis through a rotation of $\frac{\pi}{2}$, then the Hamiltonian becomes:

$$H_2 = J_1 \sum_{<ij>} S_i^x S_j^x + J_2 \sum_{<<ij>>} S_i^x S_j^x - h \sum_i S_i^z \quad (2)$$

H_2 acted on a generic spin state $(\dots \sigma_i \dots \sigma_j \dots)$ of the lattice will produce a state that has the same total number of spin ups and spin downs. Thus, exploiting this symmetry, we can block diagonalize the Hamiltonian into two blocks: one with states consisting of an even number of up spins, and one with states consisting of an odd number of up spins. This cuts down the effective size of the matrix that needs to be diagonalized by a factor of two, allowing the full Hamiltonian to be completely diagonalized. For the specific program implementation, we drew heavy inspiration from the algorithmic procedures discussed in [2]. For full diagonalization, we utilized eigen(...) from the LinearAlgebra package of the Julia programming language.

However, since we are mostly interested in the properties of the system at $T = 0$, full diagonalization is not required for most properties of interest. For the most part, obtaining the ground state and its energy will suffice. The Lanczos algorithm is an efficient diagonalization algorithm that can efficiently find a small number of the smallest or largest eigenvalues and their corresponding eigenvectors, even for matrices of extremely large sizes. This makes the Lanczos algorithm well suited for our purpose and allows us to explore systems even larger than the 4×4 lattice– for the Hamiltonian matrix of the 16-site lattice, the algorithm takes less than 2 seconds to complete. For this project, we used eigsolve(...) from Julia's KrylovKit package.

One important consideration is that the 16-site lattice contains unusual symmetries in its geometry that make its properties less representative of the infinite checkerboard lattice at low fields. We are currently applying ED techniques to a 3×8 24-site lattice, which has less of these symmetries and is more representative.

C. Numerical-Linked Clusters Method

As aforementioned, finite lattices such as the 16-site lattice can exhibit symmetries that cause properties to exhibit unusual trends, particularly at low fields. Larger lattices lose these symmetries but are also much harder to diagonalize since the Hamiltonian sizes grows exponentially with the size of the system. Thus, it is imperative that different techniques be used to calculate properties to create a comparison and gauge the effect of these symmetries. One such technique is the Numerical-Linked Cluster (NLC) Method, a method that allows one to estimate an extensive property P for an infinite lattice $\mathcal{L}$:

$$\frac{P(\mathcal{L})}{N} = \sum_c L(c) W(c) \quad (3)$$

Here, c represents the subclusters of the lattice, and $L(c)$ is the lattice constant of that subcluster (i.e. how many times the subcluster arises within the lattice). The subclusters used for the checkerboard lattice are shown in Figure. 3, chosen to be the plaquettes with the cross interactions and combinations of these plaquettes.

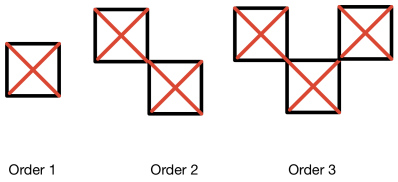

FIG. 3: The clusters of the checkerboard lattice used in the NLC method.

The weight $W(c)$ of a subcluster c is defined recursively as follows:

$$W(c) = P(c) - \sum_{s \subset c} W(s) \quad (4)$$

Where $P(c)$ is the property calculated on the subcluster c, and $s \subset c$ represent all of the subclusters of c [3].

The NLC program is currently organized so that it takes in a text file containing all of the information about the subclusters, up to subclusters consisting of a chain of six plaquettes (i.e. an NLC order of six). The program reads the data and then applies Exact Diagonalization methods to calculate the property $P(c)$ of each subcluster c, from which it generates a list of weights and runs the NLC calculation.

An important thing to note is that because we are utilizing a low finite order in our NLC calculation, the calculation does not converge well at low field (h) values. In particular, the NLC first begins to diverge at the field value where the phase transition occurs, h_c. We will see this become apparent in the results.

III. RESULTS AND DISCUSSION

Before we present the results, we'd like to establish that all exact diagonalization results were obtained using a 4×4 checkerboard lattice. In addition, any graph labelled "order x" is one produced by an NLC calculation of order x. Finally, all calculations were done on the ground state, at $T = 0$.

A. Magnetization

We first plot the results of ED and the NLC for the magnetization along the field, M, against the field h in Figure. 4. The magnetization is defined below, and it measures the extent to which the spins in the lattice are oriented parallel to the field.

$$M = \frac{1}{N} \sum_i \langle \sigma_i^x \rangle \tag{5}$$

Here, ψ refers to the state of the N-site system. σ_i^x refers to the operator representing the component of spin in the direction of the field.

Below, we plot the magnetization as a function of h for the case where $J_1 = J_2 = 1$. We expect that as the field strength is increased, more and more of the spins will begin to align with the field, and when $h >> J_1$ and $h >> J_2$, we expect that $M = \frac{1}{2}$. In Figure. 4, we see that the field asymptotically seems to approach 0.5 as the field strength is increased.

An important feature of the plot in Figure. 4 is the field at which the inflection point occurs for the results are. There can never be a true phase transition observed from the ED line (i.e. an observed discontinuity in the derivative), since the ED analysis is done on a finite system. However, the inflection point in the ED graph is still indicative of where the phase transition in the infinite system roughly is. The NLC result, however, does indicate the location of the phase transition, since it is an estimation of the property for the infinite system. In this case, however, the ED result diverges from the NLC result at around $h = 0.6$, indicating that the ED results are not indicative of the infinite system at fields below this value.

Although we have not yet determined the exact numerical value at which the inflection points occur in these graphs, a look at the NLC results gives a rough approximation of 0.2. For the ED line, we see that the inflection point occurs at a slightly higher h value, at around $h = 0.23$. We will see later on that other graphs of other properties point to the same field value for the phase transition.

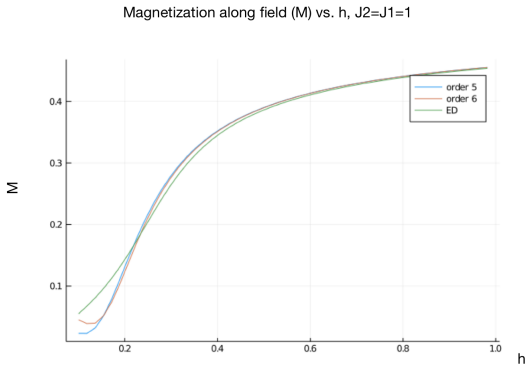

FIG. 4: The magnetization M plotted against h for the case where $J_1 = J_2 = 1$. We see all results asymptotically approach 1/2 with increasing field. In addition, we can see that the inflection point in the NLC result seems to be roughly around $h = 0.2$, indicating the field at which a phase transition occurs.

Another important takeaway from this plot is that the order 5 and 6 NLC results drastically diverge when h is extremely low. This confirms that the NLC method does not converge well at low fields, and so those results should not be trusted. However, we see that at higher fields, the NLC results agree almost perfectly, both asymptotically converging to $\frac{1}{2}$ with the increasing field, as expected. Additionally, it's worth noting that the NLC and ED results are in almost exact agreement at higher fields (at the aforementioned $h = 0.6$), which is to be expected. Both the NLC and ED predict the infinite system extremely well for high fields.

We also present Exact Diagonalization results for M when the ratio $\frac{J2}{J1}$ is varied:

The inflection points in this graph exhibit an interesting trend. We see that the inflection point of the curve of $J_2 = 0$ be at high fields, and as J_2 increases, the inflection points of their respective curves shifts back down to low fields. However, once $J_2 > J_1$, we see that the inflection points begin to shift back to the right, suggesting that the phase transition is once again occurring at higher fields. This suggests that as J_2 moves further away from 1, the phase transition shifts towards higher fields.

B. The Entanglement Entropy

The Von Neumann entanglement entropy, S_E, is a purely quantum mechanical property that measures how entangled a sublattice A is with the rest of the lattice. It is defined as follows:

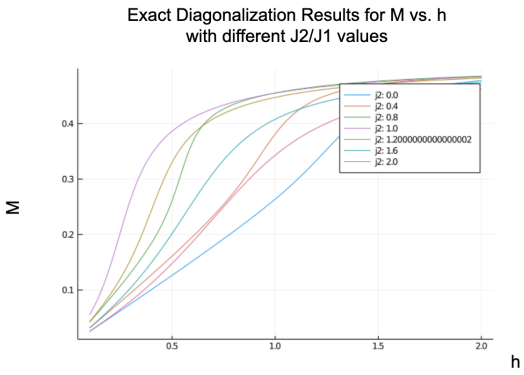

FIG. 5: The magnetization M plotted against h for the case with varying ratios of J_2/J_1. The ED was calculated using exact diagonalization methods on a 4×4 lattice.

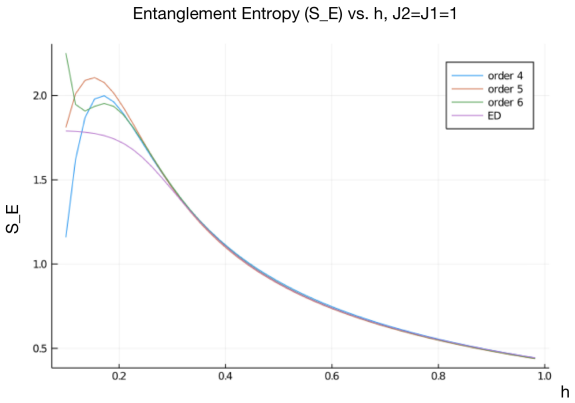

FIG. 7: The results for the entanglement entropy from the NLC and ED calculations as a function of the field. Here, $J_2 = J_1$. We see a large divergence of the NLC calculations at low fields.

$$S_E = -\operatorname{Tr}\{\rho_A \ln \rho_A\} \tag{6}$$

Where ρ_A is the reduced density matrix constructed for the subsystem A with its complement $\bar{A}$, $\rho_A = \operatorname{Tr} \bar{A}|\psi\rangle\langle\psi|$. For the checkerboard lattice, we choose the subsystem A to be a single plaquette of our lattice, highlighted below in Fig. 6.

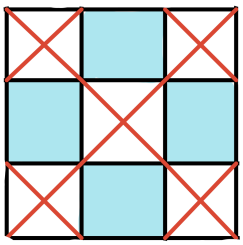

FIG. 6: The subsystem used for calculation of S_E can be any of the highlighted squares.

We present NLC and ED results for the entanglement entropy in Fig. 7.

Both the ED and the NLC results suggest that the introduction of quantum fluctuations destroys the system's high entanglement phase, where all results show the entanglement entropy sharply dropping off at high fields. An important thing to note is that the inflection point in the NLC curves here roughly aligns with where the inflection point is in the NLC M curve. This continues to strongly suggest a phase transition at around that field value. We also now note that this phase transition is accompanied by a sharp drop in the system's entanglement.

Another important takeaway from the NLC results is that its tend suggests that the entanglement entropy peaks before falling down again as h goes to 0. We know that the entanglement entropy should be lower than $\ln 6$ as h goes to 0 for reasons discussed earlier. Here, we see that the NLC results is set to exceed $\ln 6$ (as previously discussed $\ln 6$ comes from the 6 degenerate states for the classical Ising model) right before the NLC result breaks down. Thus, it suggests that S_E must peak at some value equals to or higher than $\ln 6$, then fall back down to the expected low field (h) value.

We see the ED results for S_E start around $\ln 6 \approx 1.79$. This is an expected result for the 16-site lattice. For low fields, each of the 6 states that obey the ice rules for the subsystem A should each be equally likely to occur, resulting in a high entanglement of the plaquette with the rest of the system at a value right below $\ln 6$. However, this result will not be true for lattices of higher dimension. In those systems, the superposition of the 6 states will no longer be equivalent and will favor the Néel states instead. Since we know that the entropy is maximized when the 6 states are in an equal superposition, we expect the entanglement entropy to be smaller than $\ln 6$ (In fact, $\ln 6$ is the upper limit for the checkerboard lattice's entanglement entropy when the field goes to 0).

It's worth noting that the entanglement entropy is only maximized for the 16-site lattice because the 16-site lattice exhibits many additional symmetries that larger lattices do not have. For instance, because of its small size, the sites at the ends of a diagonal drawn across the lattice are actually functionally equivalent. This also explains why many of the quantities, such as the magnetization, which we have seen earlier, become inaccurate at low fields for the ED result.

We can also further expand on and confirm this result if we plot the ED results for the entanglement entropy at a low field value, $h = 0.1$, against the ratio $\frac{J_2}{J_1}$ in Figure. 8.

For $J_2/J_1 < 1$, we see that the entanglement entropy sits at a constant value at around $\ln 2$. This reflects the fact that the ground states for the plaquette are the 2 Néel states at $h = 0$, and so at low fields we expect an equal superposition of those 2 states. Right at $J_2/J_1 = 1$, we see the entanglement entropy spiking at $\ln 6$, as we have seen before. The entanglement entropy then falls back down to $\ln 4$, since there are 4 ground

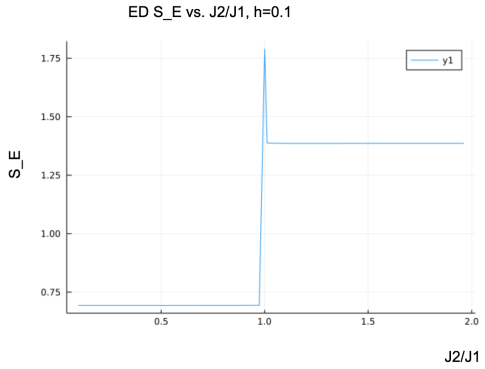

FIG. 8: The results for the entanglement entropy at low fields ($h = 0.1$) as a function of J_2/J_1. Notice the sharp jump from $\ln 2$ to $ln6$ as J_2/J_1 goes to 1, then back down to $ln4$ as J_2/J_1 further increases. This reinforces the fact that there are 2, 6, and 4 degenerate states in when $h = 0$ for each plaquette for each of the ranges of J_2/J_1.

states for the plaquette at $h = 0$ when the next nearest neighbor bonds contribute more.

When the field is increased for values of $J_2/J_1 < 1$, we see an interesting behavior where the entanglement entropy rises briefly before sharply falling off. This behavior is shown in the Figure. 9 for multiple values of J_2/J_1.

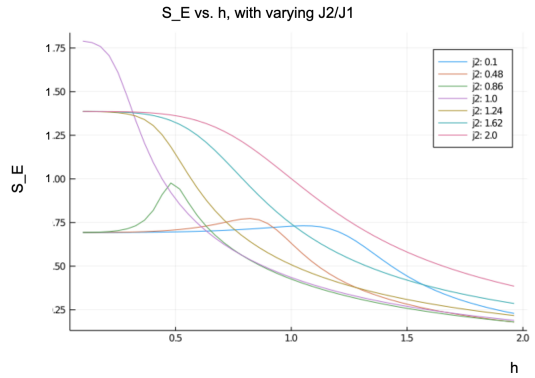

FIG. 9: The results for the entanglement entropy as a function of the field for multiple values of J_2/J_1

We suspect that the brief rise in entanglement entropy for the curves where $J_2/J_1 < 1$ indicate the point at which the effect of J_2/J_1 is not significant in comparison to that of the field. At this point, those curves begin to chase after the curve of $J_2/J_1 = 1$, approximately following its curvature for higher fields. When the field is much lower compared to J_2/J_1, however, the effects of J_2/J_1 become apparent,and so the entanglement entropy falls away from the J_2/J_1 curve, back down to $\ln 2$.

C. Néel Order Parameter

Another important quantity of interest in is the order parameter for the Néel state, $S_{\pi,\pi}$, which is defined as follows:

$$S_{\pi,\pi} = \frac{1}{N}\sum_i \sum_j \langle \sigma_i^z \sigma_j^z \rangle (-1^{i+j}) \tag{7}$$

Here, i, j span all of the sites inside the N-site lattice, where each site is assigned to have a number that's either 1 or 0. The sites are numbered in a way such that any site whose numbering is 1 will have nearest neighbors who are numbered with 0, as indicated in Fig. 10. σ_x in this case refers to the direction of the field. In the S_z basis, the field points along the x axis.

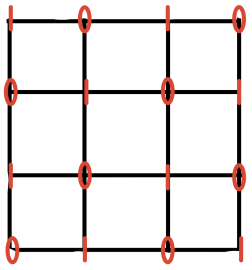

FIG. 10: The numbering of sites used in the calculation of $S_{\pi,\pi}$.

NLC calculations of different order and ED results for $S_{\pi,\pi}$ are plotted below as a function of the field for the system $J_1 = J_2$:

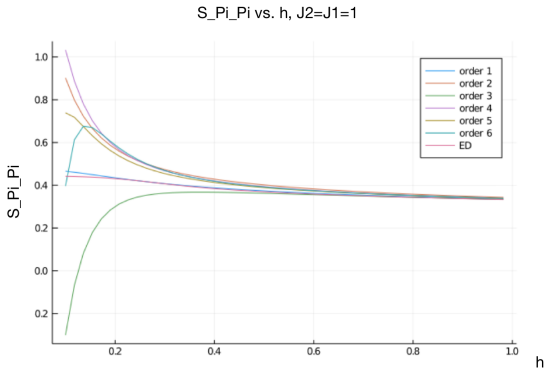

FIG. 11: The results for the $S_{\pi,\pi}$ entropy from the NLC and ED calculations as a function of the field. The ED results intersect the y axis at $S_{\pi,\pi} \approx 0.442200460$

We expect $S_{\pi,\pi}$ to be high when there is Néel order in the state. At low fields for $J_2 = J_1$, the ground state should be roughly in an equal superposition of the 6 states that obey the ice rules, including 2 that are of Néel order. The presence of these Néel states in the superposition means that we expect

the value of $S_{\pi,\pi}$ to be relatively high at low fields, reflecting the presence of those two states in the superposition. The increasing field causes the spins to align in the direction of the field. In this case, $S_{\pi,\pi}$ should drop to $\frac{1}{4}$ as the field increases, since every term in the double sum except for the case where $i = j$ will be 0. Both the NLC and ED results in Fig. 11 support the high field behavior. Before the NLC results diverge, we see that curves exhibit asymptotic convergence towards 0.25 from some higher value except for the curve at order 3, which exhibits irregular divergent behavior. The ED results reflect the predicted behavior at low fields, but in contrast to the previous quantities calculated, the NLC results don't seem to agree well until the field is extremely high ($h > 1$), and so we cannot trust it to confirm $S_{\pi,\pi}$'s behavior at low fields. We suspect that there is either i) a mistake in the $S_{\pi,\pi}$ calculation, or ii) the highly frustrated system exhibits a lot of low order fluctuations, resulting in the large divergence. The overall oddity in the NLC result for $s_{\pi,\pi}$ is currently under investigation, particularly the result for an NLC calculation of order 3.

Like the other quantities, we also plotted the ED results for $S_{\pi,\pi}$ with different values of J_2/J_1.

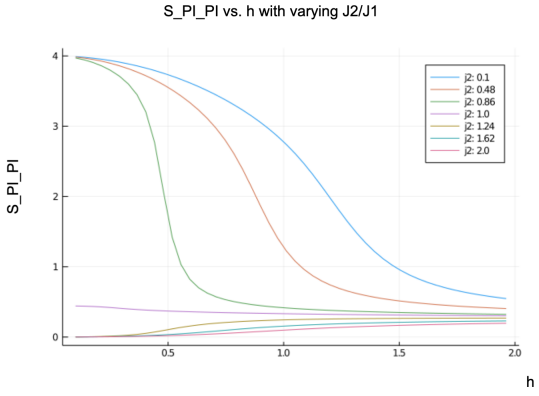

FIG. 12: The ED results for $S_{\pi,\pi}$ as a function of the field at different ratios of J_2/J_1

For $J_2 < J_1$, we see that $S_{\pi,\pi}$ starts at a very high value of 4. When the next nearest neighbors contribute less to the Hamiltonian, this means that the two Néel states are the preferred ground states when $h = 0$. Thus, when the field is low but non-zero, we expect the ground state to be in a superposition of these two Néel states, causing $S_{\pi,\pi}$ to be extremely high. This order is destroyed as the field increases, causing $S_{\pi,\pi}$ to sharply drop back down.

In contrast, when $J_2 > J_1$, $S_{\pi,\pi}$ starts near 0 and rises. We expect this behavior because at $h = 0$, this ratio of J_2/J_1 will have the ground states to be the 4 states of non-Néel order that obey the ice rules. This means that at low but nonzero fields, the ground state will be in a superposition of these non-Néel order states, meaning that $S_{\pi,\pi}$ naturally will assume a low value. As the field is increased, the spins are aligned more and more towards the x-direction, and so $S_{\pi,\pi}$ approaches 0.25, as discussed before.

D. Fidelity Susceptibility

The fidelity susceptibility χ_F is a measure of how sensitive the ground state at a particular field is to changes in the field. The fidelity is defined with an inner product of the ground state at h, $\psi(h)$, and the ground state when the field is perturbed to $h + dh$, $\psi(h + dh)$. A notable indicator of a phase transition is where the ground state changes incredibly rapidly with the field, which is reflected by peaks in the fidelity.

$$\chi_F = \frac{2(1 - |\langle\psi(h)|\psi(h + dh)\rangle|)}{dh^2} \tag{8}$$

Below, we plot the ED results for the fidelity for different values of J_2/J_1.

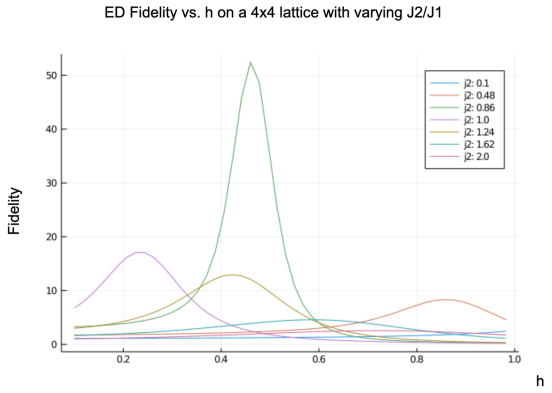

FIG. 13: The ED results for the fidelity as a function of the field at different ratios of J_2/J_1

We see the same trend in the phase transitions as J_2/J_1 is varied. The peak in the fidelity for low J_2/J_1 starts at high h, falls to a minimum when $J_2/J_1 = 1$, then rises back to higher fields as J_2/J_1 exceeds 1. This further confirms the trend of the field value at which the phase transitions occurs, where it increases as J_2/J_1 moves away from 1.

IV. CONCLUSION

The plots shown above affirm that ED and NLC methods can reproduce the expected behavior of the system as the field changes. The data from all of the calculated properties suggest that the phase transition shifts towards higher fields as J_2/J_1 moves away from 1. In addition, we see expected behavior for all of these quantities as the field and J_2/J_1 are varied. Currently, more data needs to be run for a construction of the system's phase diagram, and ongoing work is being done to obtain the necessary data.

A. Future Work

Currently, only ED has been used to calculate the fidelity. One future direction would be to utilize the NLC method to

calculate the fidelity and compare the results with those of ED.

Another area of work that could be done would be to add a correction to the NLC method so that it converges better at low fields. As it was reflected in most of the NLC results, the method does not converge well for low fields for finite order, particularly after the point where the phase transition roughly occurs. Adding a correction could make the NLC results more reliable at low fields and provide a better understanding of the infinite checkerboard lattice's behavior at lower fields.

Additionally, calculating the numerical value at which the NLC method begins to diverge at different values of J_2/J_1 would be an immediate next step to get an estimate of where the phase transition occurs and produce a phase diagram of h_c vs. J_2/J_1.

In conclusion, from the data, it appears that ED and NLC methods captures the expected behavior of the system, although much more work needs to be done in order to construct the phase diagram using these methods and draw additional conclusions.

V. ACKNOWLEDGEMENTS

I'd like to thank Dr. Rajiv Singh and Yutan Zhang for their guidance in this project. Without them, this work would not have been possible. Additionally, I'd like to thank NSF for funding this research. Finally, I'd also like to thank Dr. Rena Zieve and Dr. Nicholas Curro for organizing the REU and for their guidance throughout the summer.[4]

[1] M. Sadrzadeh, R. Haghshenas, and A. Langari, "Quantum phase diagram of two-dimensional transverse field Ising model: unconstrained tree tensor network and mapping analysis," *Physical Review B* **99**, (2019).

[2] A. W. Sandvik, "AIP Conf. Proc." **1297**, 135 (2010)

[3] Rigol, Marcos and Bryant, Tyler and Singh, Rajiv R. P., " Numerical Linked-Cluster Approach to Quantum Lattice Models" *Physical Review Letters* **97**, 135 (2006)

[4] Work done in collaboration with Yutan Zhang and Rajiv Singh, to be published